







## Molecular enhancement factors for the $\mathcal{P}$ , $\mathcal{T}$ -violating electric dipole moment of the electron in $\text{BaCH}_3$ and $\text{YbCH}_3$ symmetric top molecules

Yuly Chamorro <sup>1</sup>, Anastasia Borschevsky <sup>1</sup>, Ephraim Eliav <sup>2</sup>, Nicholas R. Hutzler <sup>3</sup>,  
Steven Hoekstra <sup>1</sup> and Lukáš F. Pašteka <sup>1,4,\*</sup>

<sup>1</sup>*Van Swinderen Institute for Particle Physics and Gravity, University of Groningen, 9747 AG Groningen, The Netherlands*

<sup>2</sup>*School of Chemistry, Tel Aviv University, 69978 Tel Aviv, Israel*

<sup>3</sup>*Division of Physics, Mathematics, and Astronomy, California Institute of Technology, Pasadena, California 91125, USA*

<sup>4</sup>*Department of Physical and Theoretical Chemistry, Faculty of Natural Sciences, Comenius University, Mlynská Dolina, 84215 Bratislava, Slovakia*



(Received 8 August 2022; accepted 1 November 2022; published 29 November 2022)

High-precision tests of fundamental symmetries are looking for the parity- ( $\mathcal{P}$ ), time-reversal- ( $\mathcal{T}$ ) violating electric dipole moment of the electron (eEDM) as proof of physics beyond the Standard Model. Particularly, in polyatomic molecules, the complex vibrational and rotational structure gives the possibility to reach high enhancement of the  $\mathcal{P}$ ,  $\mathcal{T}$ -odd effects in moderate electric fields, and with the possibility of increasing the statistical sensitivity by using laser cooling. In this work, we calculate the  $\mathcal{P}$ ,  $\mathcal{T}$ -odd molecular enhancement factor of the eEDM ( $W_d$ ) and of the scalar-pseudoscalar interaction ( $W_s$ ) necessary for the interpretation of future experiments on the promising candidates  $\text{BaCH}_3$  and  $\text{YbCH}_3$ . We employ high-accuracy relativistic coupled cluster methods and systematically evaluate the uncertainties of our computational approach. Compared to other Ba- and Yb-containing molecules,  $\text{BaCH}_3$  and  $\text{YbCH}_3$  exhibit larger  $W_d$  and  $W_s$  associated to the increased covalent character of the  $M$ -C bond. The calculated values are  $3.22 \pm 0.12 \times 10^{24} \frac{\text{hHz}}{\text{e cm}}$  and  $13.80 \pm 0.35 \times 10^{24} \frac{\text{hHz}}{\text{e cm}}$  for  $W_d$ , and  $8.42 \pm 0.29 \text{ hkHz}$  and  $50.16 \pm 1.27 \text{ hkHz}$  for  $W_s$ , in  $\text{BaCH}_3$  and  $\text{YbCH}_3$ , respectively. The robust, accurate, and cost-effective computational scheme reported in this work makes our results suitable for extracting the relevant fundamental properties from future measurements and also can be used to explore other polyatomic molecules sensitive to various violations of fundamental symmetries.

DOI: [10.1103/PhysRevA.106.052811](https://doi.org/10.1103/PhysRevA.106.052811)

### I. INTRODUCTION

The Standard Model of particle physics (SM) is known to be the most successful theory in describing the universe at the smallest scale. This model predicts all the known fundamental particles and explains their interactions via three of the four fundamental forces. However, despite its successful descriptions, SM is known to be an incomplete theory. Several well-established experimentally observed facts, such as the matter-antimatter asymmetry and the existence of dark matter [1] and dark energy [2], are not described by the SM. In particular, the matter-antimatter asymmetry requires an amount of charge-parity ( $\mathcal{CP}$ ) violation incompatible with the SM [3]. The incompleteness of the SM is both an incentive and an opportunity to look for physics beyond the Standard Model (BSM), also known as new physics.

High-precision tests of fundamental symmetries are a very effective means of probing BSM physics [4]. Specifically, precision experiments in the submicrohertz level using atoms and molecules are searching for the electric dipole moment of the electron (eEDM). The eEDM violates both time-reversal symmetry ( $\mathcal{T}$ ) and parity symmetry ( $\mathcal{P}$ ) and, assuming Charge,

Parity, and Time reversal symmetry conservation ( $\mathcal{CPT}$  theorem), the eEDM thus also violates  $\mathcal{CP}$  symmetry. In the SM, the eEDM is highly suppressed and the predicted value is far too small to be measured using current experimental techniques. This has been estimated to be of the order of magnitude of  $|d_e^{\text{SM}}| < 10^{-40}$  [5]. On the other hand, the BSM theories predict values in the experimental reach [6,7], and a measurement of a nonzero value would be an incontrovertible proof of new physics [8].

The presence of the eEDM induces an EDM on paramagnetic molecules [9,10] which is enhanced due to the internal electric fields. It has been previously shown that this enhancement grows with the atomic number as  $Z^3$  [11], making systems containing heavy atoms ideal for measuring the eEDM. Additionally, the experimental signal is also enhanced when using close-lying opposite parity states—more information can be found in the work of Sandars [12,13]. In atoms, opposite-parity electronic states are split by  $\sim 2 \text{ eV}$ , while, in molecules, opposite-parity rotational states are typically split by  $\sim 10^{-5} \text{ eV}$ . Consequently, some molecular states can offer a dramatically higher enhancement than the enhancement found in atoms [14,15]. Motivated by such enhancements, numerous experiments are being developed using molecules containing heavy atoms. The first experiments using diatomic molecules were performed on TlF in Oxford [14,16–18], and the current, most stringent result has been set in ThO by the

\*Corresponding author: [lukas.f.pasteka@uniba.sk](mailto:lukas.f.pasteka@uniba.sk)

ACME collaboration;  $|d_e^{\text{ThO}}| < 1.1 \times 10^{-29} e \text{ cm}$  [19]. Other investigated diatomic molecules include YbF [20], HfF<sup>+</sup> [21], ThO [19], RaF [22,23], and BaF [24].

Some diatomic molecules, such as PbO [25], ThO [19], and HfF<sup>+</sup> [21], have almost degenerate opposite-parity (excited) eigenstates, called  $\Omega$  doublets, which are used to measure the eEDM. These parity doublets have a small splitting which makes it possible to fully mix (or polarize) them in moderate electric fields. Additionally, the use of  $\Omega$  doublets gives the possibility to cancel many systematic effects. Unfortunately, due to the complex structure of the  $\Omega$ -doublet states, it is not possible to take advantage of laser cooling to improve the experimental sensitivity. On the other hand, measurements of the eEDM in diatomic molecules in their ground state, such as BaF [24], YbF [20,26], and RaF [23], cannot make use of the  $\Omega$ -doublet states.

Polyatomic molecules emerge as good candidates for eEDM experiments [27,28]. In contrast to diatomic molecules, in polyatomic molecules it is possible to measure the eEDM in the long-lived close-lying opposite parity eigenstates ( $K$  doublets). In addition, previous works [29–34] have discussed the feasibility of the laser cooling of metal-containing molecules composed of a single metal atom bound to a single molecular ligand, such as the symmetric top molecules BaCH<sub>3</sub> and YbCH<sub>3</sub>. This is also supported by that fact that the lighter CaCH<sub>3</sub> and MgCH<sub>3</sub> exhibit quasideagonal Frank-Condon factors [31].

The enhancement of the eEDM interaction in atoms and molecules is usually expressed in terms of the electronic structure parameter  $W_d$ . The scalar-pseudoscalar (S-PS) electron-nucleus interaction is also  $\mathcal{P}$ ,  $\mathcal{T}$  violating and enhanced in atoms and molecules. This enhancement is expressed in the electronic structure parameter  $W_s$ . Both parameters,  $W_d$  and  $W_s$ , are needed to extract the particle physics information from eEDM measurements performed in multiple systems (see, e.g., [35]). Since  $W_d$  and  $W_s$  cannot be measured experimentally, it is necessary to use electronic structure methods to calculate them.

In this work, we report the  $W_d$  and  $W_s$  parameters for the promising eEDM candidates for future experiments, the BaCH<sub>3</sub> and YbCH<sub>3</sub> molecules. Since the enhancement factor depends mainly on the identity of the heavy atom, it is expected that BaCH<sub>3</sub> and YbCH<sub>3</sub> have similar enhancement factors comparable to other isoelectronic molecules relevant for eEDM experiments, such as BaF, BaOH, and YbF, YbOH [36–39], respectively. However, unlike in the diatomic molecules BaF and YbF, the symmetric top molecules BaCH<sub>3</sub> and YbCH<sub>3</sub> have long-lived  $K$  doublets accessible to experimental measurement with an even smaller splitting than in the linear polyatomic BaOH and YbOH molecules, typically  $\leq 1$  MHz [27]. The use of these  $K$  doublets to measure the eEDM in BaCH<sub>3</sub> and YbCH<sub>3</sub> makes it possible to access large enhancement of the eEDM using moderate electric fields, reach a high experimental sensitivity, and avoid many systematic effects.

To calculate the  $W_d$  and  $W_s$  parameters, we employ high-accuracy single-reference and Fock-space coupled cluster methods and we explore the effect of the different computational factors on the calculated values. The employed methodology allows us to estimate the uncertainty in the

calculated values of  $W_d$  and  $W_s$ . The accurate and robust computational scheme established in this work may be extended to other polyatomic molecules sensitive to parity-violating effects.

## II. METHODOLOGY

The eEDM operator  $H^{\text{eEDM}}$  can be written in terms of a one-body operator [40] (here, and throughout the rest of this section, atomic units are used),

$$H^{\text{eEDM}} = 2icd_e \sum_i \gamma_i^5 \gamma_i^0 \mathbf{p}_i^2, \quad (1)$$

where  $\gamma^0$ ,  $\gamma^1$ ,  $\gamma^2$ , and  $\gamma^3$  represent the Dirac matrices,  $\gamma^5 = i\gamma^0\gamma^1\gamma^2\gamma^3$ ,  $\mathbf{p}_i$  is the momentum of the electron  $i$ , and  $c$  is the speed of light.

The S-PS interaction can be expressed as

$$H^{\text{S-PS}} = i \frac{G_F}{\sqrt{2}} Z_N k_s \sum_i \gamma_i^0 \gamma_i^5 \rho(\mathbf{r}_{iN}), \quad (2)$$

where  $G_F$  is the Fermi constant ( $2.2225 \times 10^{-14}$  a.u.),  $Z_N$  is the atomic number of the nucleus  $N$ , and  $\rho(\mathbf{r}_{iN})$  is the nuclear charge distribution. In Eqs. (1) and (2),  $d_e$  and  $k_s$  parametrize the eEDM and S-PS interaction, respectively.

To calculate the electronic structure constants  $W_d$  and  $W_s$  using the coupled cluster approach, we use the finite field method [41,42], similar to our earlier works [37,38,43–46].

The total Hamiltonian  $H$  is expressed as a sum of a zeroth-order Hamiltonian  $H^{(0)}$  and a perturbation  $H_k$ , regulated by the field strength parameter  $\lambda_k$ ,

$$H = H^{(0)} + \lambda_k H_k. \quad (3)$$

In our case,  $H^{(0)}$  is the unperturbed molecular Dirac-Coulomb Hamiltonian,

$$H^{(0)} = \sum_i [\beta_i m c^2 + c \alpha_i \cdot \mathbf{p}_i - V_{\text{nuc}}(\mathbf{r}_i)], \quad (4)$$

where  $\alpha_i$  and  $\beta_i$  are the Dirac matrices and  $V_{\text{nuc}}$  is the Coulomb potential. Considering the perturbations  $H^{\text{eEDM}}$  and  $H^{\text{S-PS}}$ ,

$$H_k = \frac{H^{\text{eEDM}}}{d_e}, \quad \frac{H^{\text{S-PS}}}{k_s}, \quad (5)$$

and applying the Hellmann-Feynman theorem, the  $W_d$  and  $W_s$  coupling constants can be calculated as the first derivatives of the energy with respect to  $\lambda_k$ ,

$$W_d = \frac{1}{\Omega} \langle \Psi_{\Omega}^{(0)} | \frac{H^{\text{eEDM}}}{d_e} | \Psi_{\Omega}^{(0)} \rangle = \frac{1}{\Omega} \frac{dE_{\Omega}(\lambda_{d_e})}{d\lambda_{d_e}} \Big|_{\lambda_{d_e}=0} \quad (6)$$

and

$$W_s = \frac{1}{\Omega} \langle \Psi_{\Omega}^{(0)} | \frac{H^{\text{S-PS}}}{k_s} | \Psi_{\Omega}^{(0)} \rangle = \frac{1}{\Omega} \frac{dE_{\Omega}(\lambda_{k_s})}{d\lambda_{k_s}} \Big|_{\lambda_{k_s}=0}, \quad (7)$$

where  $\Psi_{\Omega}^{(0)}$  is the unperturbed ground-state electronic molecular wave function and  $\Omega$  is the projection of the total electronic angular momentum on the internuclear axis.

The  $W_d$  and  $W_s$  constants are combined in the  $\mathcal{P}$ ,  $\mathcal{T}$ -odd effective Hamiltonian,  $H^{\mathcal{P},\mathcal{T}\text{-odd}}$  [47],

$$H^{\mathcal{P},\mathcal{T}\text{-odd}} = (W_d d_e + W_s k_s) \mathbf{S} \cdot \mathbf{n}, \quad (8)$$

where  $\mathbf{S}$  is the effective spin and  $\mathbf{n}$  is a unit vector oriented along the internuclear axis. Therefore, a measurement of the  $\mathcal{P}$ ,  $\mathcal{T}$ -violating energy difference on a single molecule provides us with the combined  $d_e$  and  $k_s$  and the disentanglement of the two effects requires experiments on different molecules [48].

### III. RESULTS

In this work, we assay a cost-accuracy balanced methodology that allows us to study polyatomic molecules that are promising for precision experiments, such as  $\text{BaCH}_3$  and  $\text{YbCH}_3$ , at the high-accuracy coupled cluster level. We study the effect of the treatment of relativity and electron correlation and the choice of the basis set on the optimized molecular geometries (Sec. III A) and on the calculated  $W_d$  and  $W_s$  parameters (Sec. III B). Finally, we estimate the uncertainty of the predicted  $W_d$  and  $W_s$  based on an extensive computational study within the presented methodology (Sec. III C).

All the calculations were carried out using a modified version of the DIRAC19 program [49,50], except for the scalar-relativistic (SR) calculations, where the CFOUR program [51,52] was employed. If not stated otherwise, the default settings of the corresponding codes were used. We applied both the single-reference coupled cluster with single, double, and perturbative triple excitations [CCSD(T)] [53] and the Fock-space coupled cluster (FSCC) with single and double excitations approach using sector (0,1) [54]. We used the uncontracted Dyall's relativistic basis sets [55–57] and the contracted atomic natural orbital correlation consistent ANO-RCC basis sets [58–61] of double-, triple-, quadruple-, and quintuple-zeta (for the ANO-RCC basis sets only) cardinality.

#### A. Geometry optimization

The spectroscopic properties and the geometries of the polyatomic molecules that are considered to be good candidates for measurements of  $\mathcal{P}$ ,  $\mathcal{T}$ -violating phenomena are usually not known *a priori*, meaning that any computational study of these systems should begin with a geometry optimization.

Due to the large number of electrons, geometry optimization of polyatomic molecules at the four-component coupled cluster level requires impractically high computational resources. We thus look for a compromise that allows sufficiently accurate calculations at a realistic computational cost. In the Appendix Sec. A 1, we describe the effects of the relevant computational parameters on the optimized geometry and use these investigations to select the optimal computational approach. After evaluating the effect of the treatment of relativity, use of contracted vs uncontracted basis set, and electron correlation, we conclude that a suitable methodology for reliable geometry optimizations of small polyatomic molecules is the combination of the SR-CCSD/CCSD(T) approach with the contracted ANO-RCC

TABLE I. Effect of basis set cardinality (ANO-RCC- $V_n$ ZP basis sets) on the optimized geometry of  $\text{BaCH}_3$  and  $\text{YbCH}_3$  at the SR-CCSD(T) level of theory and correlating 37 and 51 electrons, respectively. The final optimized geometries are italicized.

$n$	Ba–C (Å)	C–H (Å)	BaCH (deg)	B (MHz)
2	2.61	1.11	113	5032.81
3	2.58	1.10	113	5150.54
4	2.56	1.09	113	5211.18
5	2.55	<i>1.10</i>	<i>113</i>	<i>5270.29</i>
Expt. [62]	2.557–2.570	1.09	103–108	5211.140(86)
$n$	Yb–C (Å)	C–H (Å)	YbCH (deg)	B (MHz)
2	2.47	1.11	112	5462.06
3	2.38	1.09	111	5902.72
4	2.39	<i>1.09</i>	<i>112</i>	<i>5857.24</i>

basis sets and correlating the valence and core-valence ( $n - 1$ ) and ( $n - 2$ ) electrons.

The use of large basis sets is indispensable for taking full advantage of high-accuracy correlation methods such as coupled cluster and for getting a good quality description of the system. Table I and Fig. 1 show the convergence of the obtained geometry of the two molecules with the increase of the cardinality of the ANO-RCC basis set. In the  $\text{BaCH}_3$  molecule, the rotational constant of the optimized geometry (converged at the 5z basis set level) is 1.1% larger than the experimentally obtained rotational constant, and the optimized Ba–C bond length differs in 0.3–0.7% from the bond length estimated from the experimental rotational constants [62]. This slight difference is most likely due to the combined effects of scalar relativity and basis set contraction, as can be seen from Table X in the Appendix Sec. A 1. We evaluate the effect of this discrepancy on the  $W_d$  and  $W_s$  parameters and include it as a source of uncertainty in our reported values (see Sec. III C).

In  $\text{YbCH}_3$ , we found a faster convergence than in  $\text{BaCH}_3$ , and thus used the geometry obtained with the QZ basis set.

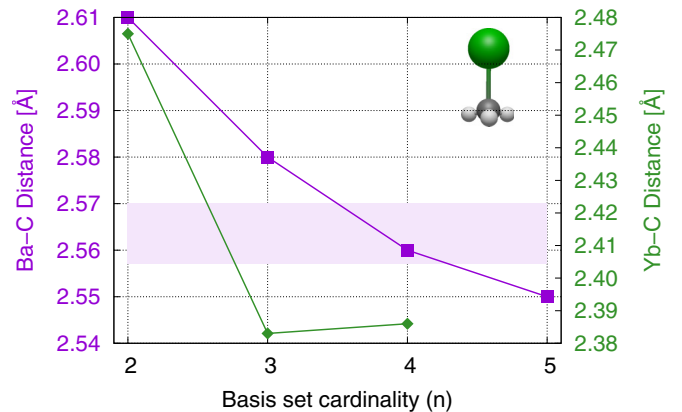


FIG. 1. Convergence of the  $M$ -C bond length ( $M$ : Ba, Yb) with basis set cardinality (ANO-RCC- $V_n$ ZP basis sets). The calculations were carried out at the SR-CCSD(T) level of theory and correlating 37 and 51 electrons, respectively. The shaded area corresponds to the experimental bond range distance Ba–C in  $\text{BaCH}_3$ .

The optimized geometries used for the calculations of the  $W_d$  and  $W_s$  parameters in the following sections are presented in italics in Table I.

### B. Enhancement factors: Computational parameters

Both the  $W_d$  and  $W_s$  factors are purely relativistic properties and, according to Schiff's theorem, in the nonrelativistic regime the atom or the molecule would not have an EDM even if the electron did [63]. However, Schiff's theorem is not valid in the relativistic regime, and atoms and molecules may express a nonzero EDM [12]. Therefore, calculations of the  $W_d$  and  $W_s$  factors should be carried out in a relativistic framework.

In this work, we use the relativistic Dirac-Coulomb four-component Hamiltonian combined with the single-reference coupled cluster approximation [53] for the calculation of the  $W_d$  and  $W_s$  factors in BaCH<sub>3</sub>, and the multireference Fock-space coupled cluster approach [54] for the corresponding calculations in YbCH<sub>3</sub>.

Earlier calculations of the electric-field gradients in YbF [64] and of  $W_d$  in YbF [37] and YbOH [38] have shown that Yb-containing molecules may present a multireference character in their ground states. In this work, we found, through the T1 diagnostic [65], that the ground state of YbCH<sub>3</sub> could indeed benefit from the Fock-space coupled cluster method. In the FSCC(0,1) approach, the starting point is the closed-shell ground state of the YbCH<sub>3</sub><sup>+</sup> molecule to which one electron is added within the correlation procedure. In this work, we added the electron to the lowest-energy  $\sigma$  orbital, thus using a minimal model space. The consideration of higher-energy orbitals through a larger model space was not shown to have a significant effect on the value of  $W_d$  in YbF and YbOH [37,38].

We apply Eqs. (6) and (7) for the calculations of both the  $W_d$  and  $W_s$  factors, using  $\lambda_{d_c} = 10^{-8}$  a.u. and  $\lambda_{k_s} = 10^{-7}$  a.u. for BaCH<sub>3</sub> and  $\lambda_{d_c} = \lambda_{k_s} = 10^{-6}$  a.u. for YbCH<sub>3</sub>. These field strengths were selected guaranteeing numerical stability as shown in the Appendix Sec. A2. In all cases, the convergence criteria of the coupled cluster energy as well as the Hartree-Fock energy were fixed in the  $1 \times 10^{-11}$ – $5 \times 10^{-11}$  a.u. range.

In the following, we present the recommended  $W_d$  and  $W_s$  values and their uncertainties and discuss the scheme we use to determine the latter, focusing separately on the various parameters that determine the quality of the calculations. Initially, we focus our study on  $W_d$  and, subsequently, we include  $W_s$  in our discussion.

#### 1. Electron correlation

In this work, we investigate the effect of various computational parameters within the relativistic coupled cluster approach on the calculated  $W_d$  and  $W_s$  factors.

*a. Correlation space.* Table II and Fig. 2 present the CCSD results obtained correlating a different number of electrons; in all these calculations, the virtual cutoff was adjusted symmetrically to the number of correlated electrons (that is, the positive-energy cutoff was taken to be of the same absolute size as the negative-energy cutoff). We observe that correlating only the outer-core-valence electrons (17 electrons in

TABLE II. Effect of the number of correlated electrons,  $N$ , on the calculated  $W_d$  constants. Error relative to the all-electrons-correlated result is presented in parentheses. Relativistic CCSD and FSCC approaches for BaCH<sub>3</sub> and YbCH<sub>3</sub>, respectively, were used, combined with the dyall.v2z basis sets.

$N$	Frozen orb.		$W_d$ ( $10^{24} \frac{h\text{Hz}}{e\text{cm}}$ )
	Ba	C	
17	[Kr]4d	[He]	3.12 (−9.1%)
27	[Kr]	[He]	3.14 (−8.7%)
37	[Ar]3d		3.28 (−4.6%)
55	[Ne]		3.34 (−2.7%)
65			3.43
$N$	Frozen orb.		$W_d$ ( $10^{24} \frac{h\text{Hz}}{e\text{cm}}$ )
	Yb	C	
29	[Kr]4d5s	[He]	12.07 (−8.9%)
31	[Kr]4d	[He]	12.60 (−5.0%)
41	[Kr]	[He]	12.46 (−6.0%)
51	[Ar]3d		12.73 (−3.9%)
79			13.25

BaCH<sub>3</sub>; Ba: 5s, 5p, 6s; C: 2s, 2p; H: 1s; and 29 electrons in YbCH<sub>3</sub>; Yb: 5p, 4f, 6s; C: 2s, 2p; H: 1s) causes relative errors of  $\sim 9\%$  compared to the value obtained when all the electrons are included in the correlation treatment. Previously, we found that correlating only outer-core-valence electrons in the isoelectronic BaF also led to an error of  $\sim 10\%$  compared to the all-electron calculation [37].

Therefore, for the recommended values, all the electrons were correlated. Note that the strong dependence on the description of the core region is unusual for most other atomic and molecular properties, such as molecular geometries or spectra.

Correlation of all the electrons in the coupled cluster approach requires the simultaneous inclusion of a proportionally large number of virtual orbitals. Notice that the symmetric virtual cutoff is  $\sim 1400$  a.u. in BaCH<sub>3</sub> and  $\sim 2300$  a.u. in YbCH<sub>3</sub>. Figure 3 and Table III present the effect of the virtual cutoff on the calculated  $W_d$ , where all the electrons are correlated. According to the results obtained using virtual cutoffs of 1000

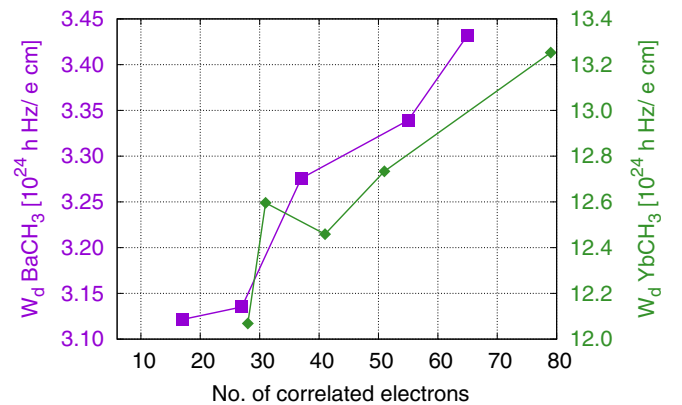


FIG. 2. Effect of the number of correlated electrons,  $N$ , on the calculated  $W_d$  constants. Values presented in Table II.



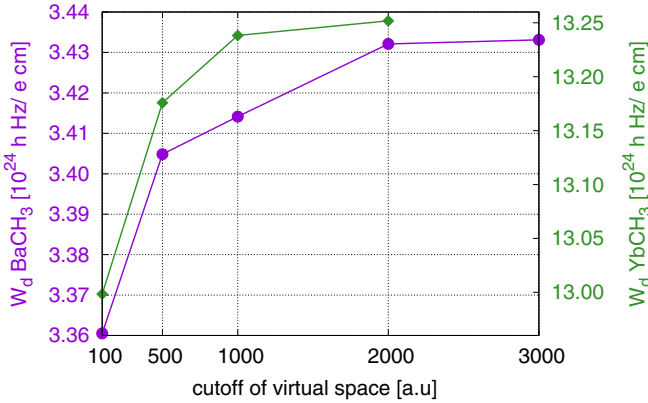


FIG. 3. Effect of the virtual space cutoff on the calculated  $W_d$  constants. Values presented in Table III.

and 2000 a.u., increasing the cutoff over 1000 a.u. changes the reported  $W_d$  by less than 0.5% for  $\text{BaCH}_3$  and by less than 0.1% for  $\text{YbCH}_3$ . In fact,  $W_d$  in  $\text{BaCH}_3$  changes by only 0.03% when the virtual cutoff is further increased to 3000 a.u. Therefore, we include all the virtual orbitals until 2000 a.u. in our recommended values, and we use the difference between the results obtained with a virtual cutoff of 2000 and of 1000 a.u. to estimate the uncertainty from neglecting virtual orbitals above 2000 a.u. in the description of the electron correlation. Furthermore, we conclude that when computational resources are a bottleneck, a lower cutoff of 500 a.u. can be used, without notable deterioration of the quality of the results.

*b. Excitation rank.* The results discussed so far were obtained at the coupled cluster (either single-reference or Fock-space) level of theory with single and double excitations.

We evaluated the effect of triple excitations comparing the calculated  $W_d$  of  $\text{BaCH}_3$  at the CCSD and CCSD(T) levels using the 2z, 3z, and 4z quality basis sets (Table IV). In all the cases, the inclusion of triple excitations slightly reduces the calculated  $W_d$ . The contribution of the triple excitations increases with the cardinality of the basis set, as expected, but even at the 4z basis set, cardinality reaches only 1.3%. The magnitude of this contribution is close to what was observed in previous calculations on  $\text{BaOH}$  (1.4%) and  $\text{BaF}$  (1.5%) and suggests that the triple excitations can be neglected when the

TABLE III. Effect of the virtual space cutoff on the calculated  $W_d$  constants. Error relative to the highest virtual cutoff value is presented in parentheses. Relativistic CCSD and FSCC approaches for  $\text{BaCH}_3$  and  $\text{YbCH}_3$ , respectively, were used, combined with the dyall.v2z basis sets. All electrons were correlated.

Cutoff (a.u.)	$W_d$ ( $10^{24} \frac{\text{hHz}}{\text{e cm}}$ )	
	$\text{BaCH}_3$	$\text{YbCH}_3$
100	3.36 (−2.1%)	13.00 (−1.9%)
500	3.41 (−0.8%)	13.18 (−0.6%)
1000	3.42 (−0.5%)	13.24 (−0.1%)
2000	3.43 (−0.03%)	13.25
3000	3.43	

TABLE IV. Effect of inclusion of triple excitations on the calculated  $W_d$  constants. The relative error of CCSD comparing to the perturbative CCSD(T) is presented in parentheses. 17 electrons were correlated and the virtual cutoff was set to 30 a.u.

Basis set	$W_d \text{ BaCH}_3$ ( $10^{24} \frac{\text{hHz}}{\text{e cm}}$ )	
	CCSD	CCSD(T)
dyall.v2z	3.12 (+0.6%)	3.10
dyall.v3z	3.01 (+1.0%)	2.98
dyall.v4z	2.95 (+1.3%)	2.91

computational resources are an issue. We report the final  $W_d$  and  $W_s$  at the CCSD(T) level and use the triples contribution to estimate the uncertainty due to neglecting higher-order excitations.

The use of the FSCC approach allows us to obtain accurate values of  $W_d$  and  $W_s$  in an open-shell system such as  $\text{YbCH}_3$ . However, as perturbative triple excitations are not yet implemented in the FSCC module of the DIRAC program, we cannot use this method to perform a reliable calculation of the contribution of the triple and higher-order excitations. Therefore, we do use the difference between the single-reference CCSD and CCSD(T) results in  $\text{BaCH}_3$  to estimate the relative uncertainty due to the neglect of the triple excitations in the  $\text{YbCH}_3$  molecule.

## 2. Basis sets

Next to the electron correlation, the quality of the basis set plays a crucial role in an accurate theoretical description of molecular properties. In the following sections, we analyze the effect of the cardinality and the special features of the basis sets on the calculated  $W_d$  and  $W_s$  factors.

*a. Complete basis set limit.* Table V presents the dependence of the calculated  $W_d$  constants on the cardinality of the basis set. Overall,  $W_d$  changes monotonically with an increase of the basis set cardinality. In  $\text{BaCH}_3$ , it decreases by 6.5%

TABLE V. Effect of the basis set cardinality ( $vnz$ ,  $n = 2, 3, 4$ ) on the  $W_d$  constants calculated using CCSD(T) with 17 correlated electrons and a virtual space cutoff of 30 a.u. for  $\text{BaCH}_3$  and using FSCC with 29 electrons correlated and virtual space cutoff of 10 a.u. for  $\text{YbCH}_3$ . In the lower part of the table, the results obtained using the different CBS extrapolation schemes and the respective uncertainty estimation are shown. Relative errors with respect to the CBS(H) limit are shown in parentheses.

Basis set	$W_d$ ( $10^{24} \frac{\text{hHz}}{\text{e cm}}$ )	
	$\text{BaCH}_3$	$\text{YbCH}_3$
dyall.v2z	3.10 (+8.3%)	12.07 (−4.4%)
dyall.v3z	2.98 (+4.1%)	12.52 (−0.8%)
dyall.v4z	2.91 (+1.7%)	12.58 (−0.4%)
CBS(M)	2.87 (+0.3%)	12.62 (−0.1%)
CBS(H)	2.86	12.63
CBS(L)	2.85 (−0.4%)	12.64 (+0.1%)
95% c.i.	0.02	0.02

TABLE VI. Effect of the basis set on the calculated  $W_d$  constants. The deviations relative to the dyall.v3z basis set are shown in parentheses. CCSD(T) level of theory with 37 electrons correlated and virtual space cutoff of 60 a.u. for BaCH<sub>3</sub> and FSCC with 31 electrons correlated and virtual space cutoff of 20 a.u. for YbCH<sub>3</sub>.

Basis set	$W_d$ ( $10^{24} \frac{\text{hHz}}{\text{ecm}}$ )	
	BaCH <sub>3</sub>	YbCH <sub>3</sub>
dyall.v3z	3.20	12.87
dyall.cv3z	3.26 (+1.71%)	12.88 (+0.05%)
dyall.ae3z	3.26 (+1.68%)	12.86 (−0.08%)
aug-dyall.v3z	3.15 (−1.74%)	12.87 (−0.02%)

when going from the 2z to 4z cardinality basis set, while in YbCH<sub>3</sub>, it increases by 4.1%. We extrapolate our results to the complete basis set (CBS) limit, using the usual three-point Dunning-Feller  $e^{-\alpha n}$  scheme ( $n = 2, 3, 4$ ) [66,67] for extrapolating the Dirac-Hartree-Fock (DHF) energies and the two-point Helgaker *et al.*  $n^{-3}$  scheme ( $n = 3, 4$ ) [68] for extrapolating the correlation energies. We also tested the Martin  $(n + \frac{1}{2})^{-4}$  scheme [69] and the recent scheme of Lesiuk and Jeziorski (based on the application of the Riemann  $\zeta$  function) [70] for extrapolating the correlation energies. The latter three extrapolation schemes (labeled H, M, and L in Table V, respectively) give evenly spread and very similar CBS limits. We use the central Helgaker CBS limit for our final results and the respective 95% confidence interval ( $1.96\sigma$ ) based on the spread of the three schemes as our extrapolation uncertainty estimate. The same methodology was used in our previous studies [71].

*b. Core correlating and diffuse functions.* The results shown in Table VI showcase the effects of including outer- and inner-core correlating (cv3z, aev3z) and diffuse (aug-v3z) functions on the calculated  $W_d$  factors. The difference between the cv3z/ae3z basis set and the v3z basis set lies in the addition of tight functions with high angular momentum, namely, 2/5  $f$  and 1/2  $g$  functions for a Ba atom and 1/1  $d$  function for C. On the other hand, the difference between the aug-v3z and the v3z lies in the even-tempered addition of diffuse functions for each angular momentum in all the atoms. For BaCH<sub>3</sub>, the two augmentation schemes cause changes that are similar in magnitude but opposite in sign, leading to a negligible net effect. The  $W_d$  in YbCH<sub>3</sub> shows a negligible dependence on both types of augmentation. In this case, the difference between the dyall.v3z and the dyall.cv3z basis sets is small since the two sets are identical for Yb and the only differences are in the number of the core-correlating functions on carbon. In the dyall.ae3z basis set for Yb, only one extra  $g$  function is added to the dyall.cv3z basis. Due to the small (and opposite) effects, we proceed with the nonaugmented dyall.v3z basis sets for both molecules and we include the effect of the augmentation and including correlating functions in our uncertainty estimation. The effect of adding tight  $d$  functions in an all-electron calculation of  $W_d$  and  $W_s$  has shown to be  $<0.3\%$  in BaF [37]; therefore, additional  $d$  functions were not included in our calculations.

### C. Recommended values and uncertainty estimation

The extensive computational study carried out in the previous section allows us to determine the most suitable method for obtaining the recommended values of the  $W_d$  and the  $W_s$  constants of the two molecules.

For BaCH<sub>3</sub>, we provide the final value of  $W_d$  calculated at the CCSD(T) level of theory using the dyall.v3z basis set, correlating all the electrons and including virtual orbitals up to 2000 a.u. giving the base value of  $3.33 \times 10^{24} \frac{\text{hHz}}{\text{ecm}}$ . To this, we add the CBS extrapolation correction of  $-0.11 \times 10^{24} \frac{\text{hHz}}{\text{ecm}}$  evaluated correlating 17 electrons with a virtual space cutoff of 30 a.u. We estimated the uncertainty due to the finite basis set (cardinality, core-correlating, and diffuse basis functions) and due to the neglect of higher-order excitations based on the study in the previous sections. To determine the size of each source of error, we use the difference in  $W_d$  obtained with the final method and  $W_d$  obtained with a lower approximation (for a given computational parameter) as schematically shown in Table VII. In addition, to estimate the uncertainty stemming from the molecular geometry optimization, we calculated the  $W_d$  factor using the experimental geometry range (Ba–C bond distance = 2.557–2.570 Å [62]) and found that the maximum variation with respect to the value obtained using the optimized geometry is 1.08%. Finally, the Dirac-Coulomb Hamiltonian used in this work assumes an instantaneous (nonrelativistic) electron-electron interaction. The Breit interaction is the first-order correction and, as it contains two-electron operators [72], it is not possible to separate this effect from the electron correlation effects. While aware of this limitation, we evaluate the effect of the dominant Gaunt term of the Breit interaction [73] at the Dirac-Hartree-Fock (DHF) level of theory, resulting in a decrease in  $W_d$  of 1.8%. We thus set an estimate of the uncertainty on our recommended values due to the missing Breit interaction and higher-order effects to 1.8%. All the individual contributions to the uncertainty are summarized in Table VII and we estimate the total uncertainty (assuming the effects are independent) at 3.44%. The recommended value for BaCH<sub>3</sub> is thus  $W_d = 3.224 \pm 0.111 \times 10^{24} \frac{\text{hHz}}{\text{ecm}}$ .

For YbCH<sub>3</sub>, we provide the final value of  $W_d$  calculated at the FSCC level of theory, correlating all the electrons and including virtual orbitals up to 2000 a.u., as we did in BaCH<sub>3</sub>. In YbCH<sub>3</sub>, however, it was computationally unfeasible to correlate all the electrons when using the dyall.v3z basis. Nevertheless, since the effect of the correlation space is bigger than the effect of the size of the basis set, we employed the dyall.v2z basis set to obtain the base value of  $13.25 \times 10^{24} \frac{\text{hHz}}{\text{ecm}}$  and to this we added the CBS correction of  $+0.56 \times 10^{24} \frac{\text{hHz}}{\text{ecm}}$ , and evaluated correlating 29 electrons with a virtual space cutoff of 10 a.u. We used an analogous scheme to that employed for BaCH<sub>3</sub> to estimate the uncertainty of this result. However, since the experimental geometry is yet not known for YbCH<sub>3</sub>, we use the same relative uncertainty due to the geometry optimization as we derived for BaCH<sub>3</sub>. This assumption is justified by the fact that we used the same methodology to optimize the geometry of the two molecules. Furthermore, to estimate the effect of the excitation rank, we include in our uncertainty estimation twice the relative uncertainty obtained

TABLE VII. Summary of the most significant sources of uncertainty in  $W_d$  in  $\text{BaCH}_3$  and  $\text{YbCH}_3$  ( $10^{24} \frac{\text{hHz}}{\text{ecm}}$ ). Values in parentheses represent the relative uncertainties with respect to the final results.

Source of uncertainty		$\delta_i W_d$ ( $10^{24} \frac{\text{hHz}}{\text{ecm}}$ ) (%)		Scheme
		$\text{BaCH}_3$	$\text{YbCH}_3$	
Correlation	Virtual cutoff	0.017 (0.5%)	0.014 (0.1%)	2000–1000 a.u.
	Triples	0.029 (0.9%)	0.252 (1.8%)	CCSD(T)-CCSD
Basis set	CBS extrapolation	0.021 (0.7%)	0.020 (0.15%)	1.96 $\sigma$
	Diffuse functions	0.055 (1.7%)	0.003 (0.02%)	aug-v3z–v3z
	Core-correl. functions	0.055 (1.7%)	0.010 (0.07%)	ae3z–v3z
Geometry	Optimization	0.037 (1.2%)	0.160 (1.2%)	opt.-expt.
Relativity	Gaunt	0.057 (1.8%)	0.180 (1.3%)	Gaunt-DC–DC
Total uncertainty		0.111 (3.44%)	0.349 (2.53%)	$\sqrt{\sum_i \delta_i^2}$
Final recommended value		$3.224 \pm 0.111$	$13.799 \pm 0.349$	

for  $\text{BaCH}_3$  to account for neglecting both the triples and the higher-order excitations. The recommended value for  $\text{YbCH}_3$  is thus  $W_d = 13.799 \pm 0.349 \times 10^{24} \frac{\text{hHz}}{\text{ecm}}$ .

Figure 4 presents the relative uncertainties for the different sources discussed above and calculated as described in Table VII. The highest contributions to the total uncertainty in  $\text{BaCH}_3$  are due to the basis set incompleteness and the current limitation to describing the Breit interaction correctly. Notice that the addition of diffuse and extra correlating functions have an opposite effect, meaning that we somewhat overestimate this source of uncertainty. In the case of  $\text{YbCH}_3$ , the employed basis set is highly converged. Consequently, the total uncertainty in  $W_d$  is smaller for  $\text{YbCH}_3$  than for  $\text{BaCH}_3$ , with the leading source of uncertainty coming from the electron correlation description.

We have also performed calculations of the  $W_s$  parameters using the computational scheme employed for the recommended  $W_d$  values. The different computational parameters included in the uncertainty estimation in this work have effects of the same magnitude on the calculated  $W_d$  and  $W_s$  in  $\text{BaF}$

[37], with the Gaunt term being the only exception. In  $\text{BaF}$ , the Gaunt term, and therefore, the total uncertainty, is smaller in  $W_s$  than in  $W_d$ . Consequently, in this work, we assume that the relative uncertainty of the  $W_s$  values is of the same order of magnitude as the uncertainty found for the corresponding  $W_d$  factors. All the recommended values are summarized in Table VIII and compared to the earlier predictions for similar molecules.

#### D. Comparison and molecular bond analysis

The final calculated enhancement factors in  $\text{BaCH}_3$  and  $\text{YbCH}_3$  are of the same order of magnitude as in their corresponding isoelectronic linear molecules  $\text{BaOH}$ ,  $\text{BaF}$ ,  $\text{YbOH}$ , and  $\text{YbF}$ , and the nonlinear polyatomic molecules  $\text{BaOCH}_3$  and  $\text{YbOCH}_3$ , respectively. However, the enhancement factors in  $\text{BaCH}_3$  and especially in  $\text{YbCH}_3$  are larger than in the other molecules.

To investigate the origin of this difference, we calculated the  $W_d$  and  $W_s$  parameters for all the systems using the same approach and used the quantum theory of atoms in molecules (QTAIM) [76] and the natural bond orbital (NBO) [77] anal-

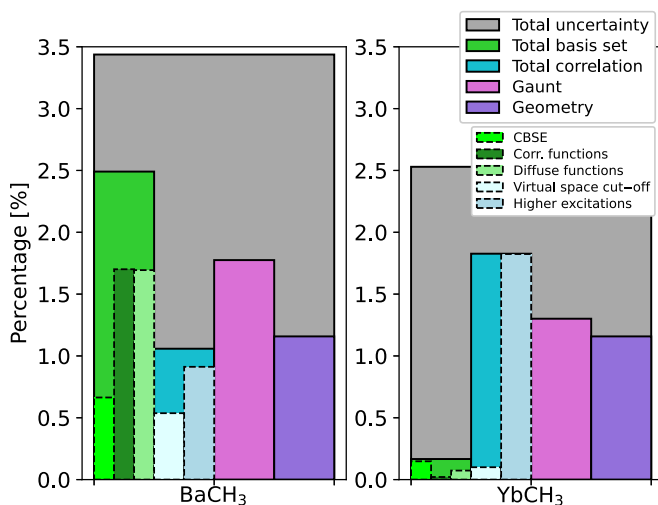


FIG. 4. Total and individual contributions to the uncertainty in percent relative to the recommended values: DC-CCSD(T), CBSE-corrected, and DC-FSCC, CBSE-corrected for  $\text{BaCH}_3$  and  $\text{YbCH}_3$ , respectively.

TABLE VIII. Recommended  $W_d$  and  $W_s$  values of  $\text{BaCH}_3$  and  $\text{YbCH}_3$  (italicized) and comparison to homologous molecules. A factor of 0.4835 was used to convert  $E_{\text{eff}}$  in  $\text{GV/cm}$  units to  $W_d$  in  $10^{24} \frac{\text{hHz}}{\text{ecm}}$  units when necessary.

Molecule	Method	$W_d$ ( $10^{24} \frac{\text{hHz}}{\text{ecm}}$ )	$W_s$ ( $h\text{kHz}$ )
<i>BaCH<sub>3</sub></i>	DC-CCSD(T)	$3.22 \pm 0.12$	$8.42 \pm 0.29$
<i>BaOCH<sub>3</sub></i>	X2C-CCSD(T)	3.05 [74]	
<i>BaOH</i>	DC-CCSD(T)	$3.10 \pm 0.15$ [38]	
	ZORA-cGHF	$3.32 \pm 0.33$ [39]	$8.79 \pm 0.88$ [39]
	ZORA-cGKS	$2.98 \pm 0.30$ [39]	$7.91 \pm 0.79$ [39]
<i>BaF</i>	DC-CCSD(T)	$3.13 \pm 0.12$ [37]	$8.29 \pm 0.12$ [37]
<i>YbCH<sub>3</sub></i>	DC-FSCC(0,1)	$13.80 \pm 0.35$	$50.16 \pm 1.27$
<i>YbOCH<sub>3</sub></i>	X2C-CCSD(T)	11.60 [74]	
<i>YbOH</i>	DC-FSCC(0,1)	$11.30 \pm 0.5$ [38]	
	ZORA-cHFS	$11.40 \pm 1.14$ [39]	$41.2 \pm 4.12$ [39]
	ZORA-cGKS	$8.54 \pm 0.85$ [39]	$30.8 \pm 3.08$ [39]
	DC-CCSD	$11.47 \pm 0.68$ [75]	
<i>YbF</i>	DC-FSCC	$11.39$ [37]	

TABLE IX. Correlation between the  $W_d$  and  $W_s$  values of interest with bonding characteristics of the  $M$ - $X$  bond ( $M = \text{Ba}, \text{Yb}$ ;  $X = \text{C}, \text{O}, \text{F}$ ). Espinoza criterion  $\frac{|V(\mathbf{r}_c)|}{G(\mathbf{r}_c)}$  is a measure of covalent bond character.  $q_M$  represents the natural charge of the heavy element.

System	$W_d$ ( $10^{24} \frac{\text{hHz}}{\text{e.u.}}$ )	$W_s$ ( $\text{hkHz}$ )	$\frac{ V(\mathbf{r}_c) }{G(\mathbf{r}_c)}$	$q_M$
BaCH <sub>3</sub>	3.10	7.60	1.64	0.78
BaOCH <sub>3</sub>	2.79	6.88	1.20	0.88
BaOH	2.82	6.96	1.22	0.90
BaF	2.80	6.89	1.28	0.89
YbCH <sub>3</sub>	12.07	41.20	1.48	0.68
YbOCH <sub>3</sub>	9.89	33.98	1.12	0.82
YbOH	10.03	34.51	1.13	0.84
YbF	10.30	35.43	1.15	0.83
YbH	13.15	45.05	1.55	0.64

yses to study the relevant bonds. Table IX presents  $W_d$  and  $W_s$  obtained at the CCSD(T) and FSCC(0,1) level for the Ba- and Yb-containing molecules, respectively. To conserve computational effort, the dyall.v2z basis set was used and a cutoff was set at  $-2$  to  $+10$  a.u. for Ba-containing and  $-1$  to  $+10$  a.u. for Yb-containing systems. For the QTAIM and NBO analysis, we employ the SR-ZORA Hamiltonian with the PBE0 functional [78] and the QZ4P basis set in the Amsterdam density functional (ADF) package [79].

In the QTAIM analysis, intermolecular interactions can be characterized according to the topology of the electron density at the bond critical points (BCPs) denoted by  $\mathbf{r}_c$ . Specifically, the criteria of Espinoza and co-workers [80] classify the bonding interactions according to the ratio of the potential  $V(\mathbf{r}_c)$  and kinetic  $G(\mathbf{r}_c)$  energy density at the BCPs,  $|V(\mathbf{r}_c)|/G(\mathbf{r}_c)$ . Ratios  $<1$  correspond to long-range, ionic or hydrogen bonds, values between  $1$ – $2$  to intermediate bonds (with both ionic and covalent character), and ratios  $>2$  to covalent bonds. The ratio  $|V(\mathbf{r}_c)|/G(\mathbf{r}_c)$  in Table IX suggests that the  $M$ - $X$  ( $M = \text{Ba}, \text{Yb}$ ;  $X = \text{C}, \text{O}, \text{F}$ ) bonds cannot be characterized as purely ionic bonds, and especially the  $M$ - $C$  bonds have a significantly increased covalent character as compared to the  $M$ - $O$  and  $M$ - $F$  bonds. The natural charges based on natural atomic orbitals (NAOs) of the heavy atoms  $q_M$  support this observation. The  $M$ - $C$  bonds are less polar compared to the  $M$ - $O$  and  $M$ - $F$  bonds. It means that in BaCH<sub>3</sub> and YbCH<sub>3</sub> molecules, the unpaired electron that experiences the  $\mathcal{P}, \mathcal{T}$ -odd interaction is more localized on the heavy atom, leading to a higher enhancement factor than for the other Ba- and Yb-containing molecules. We tested this conjecture by including YbH in our analysis, which follows the expected trend—the less electronegative hydrogen leads to more covalent bonding and an increase in the  $W_d$  and  $W_s$  values. A similar observation was made in previous works [81,82].

#### IV. EXPERIMENTAL CONSIDERATIONS

BaCH<sub>3</sub> and YbCH<sub>3</sub> are both prime candidates for the creation of intense beams via buffer gas cooling [83]. The

rotational spectrum of the ground electronic state of BaCH<sub>3</sub> has been studied via millimeter and submillimeter absorption [62] and was created via the reaction of barium metal with Sn(CH<sub>3</sub>)<sub>4</sub>. Other alkaline-earth monomethyl molecules have been created via the reaction of metals with other monomethyl species [84], including chloromethane (CH<sub>3</sub>Cl) which could be used to react with ablated Yb or Ba metal in a cryogenic buffer gas cell. While YbCH<sub>3</sub> has not been studied spectroscopically, the chemical similarity of Yb with the alkaline-earth metals means that these production methods would likely work as well, as has been demonstrated with a number of other Yb-containing molecules [34,85].

The  $\mathcal{P}, \mathcal{T}$ -violation measurement with these species would be performed in the  $K = 1$  rotational state of the ground electronic and vibrational state, in which  $K$  doubling splits the rotational states into doublets of opposite parity [27,34,86]. The state with  $K = 1$  corresponds to the molecule rotating about its  $C_{3v}$  symmetry axis with one quantum of angular momentum. Alkaline-earth metals bound to  $-\text{CH}_3$  and  $-\text{OCH}_3$  ligands have this state at roughly 160 GHz above the ground state [86–88], giving them lifetimes estimated to be minutes or longer. As this energy corresponds to  $\approx 8$  K, there will be an appreciable population in a buffer gas source at a few Kelvin. The doubling in small, open-shell molecules with a metal-centered electron and a CH<sub>3</sub> group is dominated by anisotropic dipole-dipole interactions between the H nuclear spins and unpaired electron spin [34,89]. For CaOCH<sub>3</sub>, this has been measured to be around 300 kHz [89], but, due to the closer distance between the metal and H<sub>3</sub> group in MCH<sub>3</sub> molecules, this value is likely a few times larger, around 1 MHz. Note that the overall level structure, including the states which would be used for a spin precession measurement, are similar to other symmetric top molecules [86]. Also similar is that the EDM sensitivity would saturate to  $\approx 50\%$  of the maximum values at the small fields required to mix the parity doublets [86,90].

#### V. CONCLUSIONS

In this work, we report the enhancement factors  $W_d$  and  $W_s$  needed for the interpretation of possible eEDM measurements on the promising molecules BaCH<sub>3</sub> and YbCH<sub>3</sub>. We carried out a systematic study to devise a computationally feasible scheme that provides accurate predictions along with realistic uncertainties.

We showed that the scalar-relativistic level of theory in combination with the coupled cluster method and the ANO-RCC basis sets is a feasible and accurate approach for the optimization of small polyatomic molecules. Correlating the valence and core-valence ( $n - 1$ ) and ( $n - 2$ ) electrons gives essentially the same results as correlating all electrons. The geometry obtained with this approach is in a very good agreement with the available experimental reports (for BaCH<sub>3</sub>).

The values of  $W_d$  and  $W_s$  calculated in this work for both BaCH<sub>3</sub> and YbCH<sub>3</sub> are slightly larger than in other Ba- and Yb-containing molecules. The relation between the increased covalent character of the heavy atom bond and the size of the



$W_d$  and  $W_s$  factors provides important insight in the search for promising candidates for precision experiments.

Accurate calculations of the properties needed for interpretation of precision measurements in polyatomic molecules are a challenging task and it is necessary to methodically evaluate the effects of the most relevant computational parameters. In this work, we provide such analysis for the  $\text{BaCH}_3$  and  $\text{YbCH}_3$  molecules. We show that calculating the  $W_d$  and  $W_s$  values requires an accurate description of the electron correlation. Specifically, in the coupled cluster approach, the number of electrons included in the correlation description plays the most significant role. The size of the basis set has a comparatively smaller but non-negligible effect. The systematic evaluation of the effect of various computational parameters also allowed us to estimate the uncertainty in the values presented in this work.

## ACKNOWLEDGMENTS

This publication is part of the project *High Sector Fock Space Coupled Cluster Method: Benchmark Accuracy Across the Periodic Table* [with Project No. VI.Vidi.192.088 of the research programme Vidi which is financed by the Dutch Research Council (NWO)]. We thank the Center for Information Technology of the University of Groningen for support and for providing access to the Peregrine high performance computing cluster. L.F.P. acknowledges the support from the Slovak Research and Development Agency (Grants No. APVV-20-0098 and No. APVV-20-0127).

## APPENDIX

### 1. Geometry optimization

#### a. Treatment of relativity

Relativistic effects play an indispensable role in the correct description of molecules containing heavy elements. However, inclusion of just the scalar-relativistic effects is often sufficient to describe properties that are not very sensitive to the spin components, such as molecular geometry. This, of course, holds only for systems where the spin-orbit effects are not expected to be significant for the valence electrons, such as closed-shell molecules or systems with valence  $s/\sigma$  orbitals. We test this assumption by comparing the geometries of  $\text{BaCH}_3$  obtained within the four-component (4c) and the exact two-component (X2C) [91,92] approaches and using the spin-free exact two-component one-electron variant formalism (SR) [93]. The first two methods were employed within the DIRAC19 program, while the SR calculations were performed using the CFOUR package. In Table X, it is observed that the X2C approach predicts the same results as the Dirac-Coulomb 4c Hamiltonian. Similarly, the SR calculations differ in only 0.5% to the 4c and X2C results. Consequently, the use of the computationally less expensive SR level of theory is justified in the geometry optimization of  $\text{BaCH}_3$  and  $\text{YbCH}_3$  and similar molecules.

#### b. Contracted vs uncontracted basis set

In electronic structure calculations, contracted basis functions constructed from Gaussians perform for many properties

TABLE X. Effect of the different levels of treatment of relativity on the optimized geometry of  $\text{BaCH}_3$  at the CCSD level of theory. In all cases, 37 electrons were correlated.

Rel.	Basis set	Ba-C (Å)	C-H (Å)	BaCH (deg)
4c	dyall.v2z	2.670	1.110	113.6
X2C	dyall.v2z	2.670	1.110	113.6
SR	dyall.v2z	2.657	1.108	113.2
SR	ANO.VDZ	2.613	1.107	112.7
X2C	dyall.v3z	2.605	1.100	112.8
SR	ANO.VTZ	2.585	1.098	112.6

with similar accuracy, but with dramatically reduced computational costs compared to uncontracted basis sets. In the geometry optimization of  $\text{BaCH}_3$  and  $\text{YbCH}_3$  (Table X), we observe that the scalar-relativistic approximation introduces a smaller error compared to the effect of the basis set contraction. The difference between the results obtained using contracted ANO-RCC.VDZ and uncontracted dyall.v2z basis sets at the SR level is 1.7%. However, this difference is reduced to 0.8% when comparing the larger SR-ANO-RCC.VTZ and X2C-dyall.v3z methods. This is expected since, with the increasing cardinality, the basis sets become more saturated and thus the negative effect of contraction should decrease. We thus proceed with the computationally less expensive ANO-RCC basis sets. Based on the results in Table X, when selecting basis sets for geometry optimizations considering their cost-benefit values, it is advisable to choose a higher cardinality contracted basis set over an uncontracted but lower cardinality one.

#### c. Electron correlation

Table XI contains comparison between the results obtained within the CCSD and the CCSD(T) approaches. The calculations were carried out within the single-reference framework and 37 electrons were correlated. We observe that inclusion

TABLE XI. Effect of the perturbative triple excitations on the optimized geometry of  $\text{BaCH}_3$ , at the SR level of theory.  $N$  represents the number of correlated electrons.

Method	$N$	Ba-C (Å)	C-H (Å)	BaCH (deg)
			ANO-RCC.VDZ	
CCSD	37	2.613	1.107	113
CCSD(T)	37	2.609	1.109	113
			ANO-RCC.VTZ	
CCSD	37	2.586	1.098	113
CCSD(T)	37	2.579	1.099	113
CCSD(T)	65	2.578	1.099	113
CCSD(T)	27	2.591	1.102	113
CCSD(T)	17	2.606	1.102	113

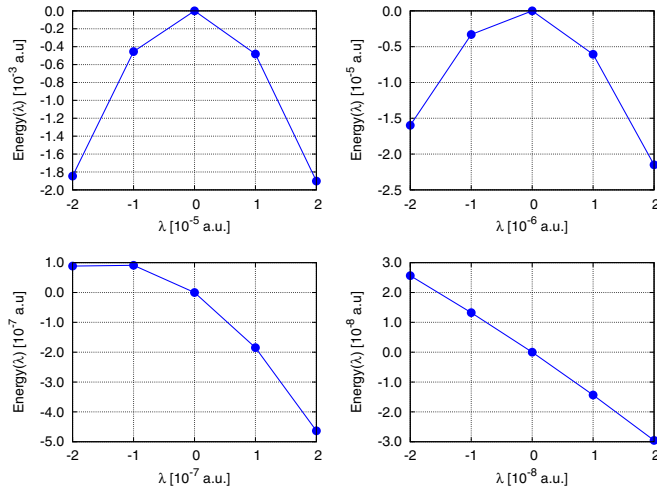


FIG. 5. Energy dependency with the field strength in  $\text{BaCH}_3$ . The 4c-CCSD and dyall.v2z basis sets were used.

of perturbative triple excitations has a minor effect on the obtained geometry (0.2% and 0.3% at the DZ and TZ basis set

cardinality, respectively) and thus conclude that optimization on the CCSD level is of sufficient quality when computational resources are of importance.

Furthermore, as expected, we find that the molecular geometry is a property mainly dependent on the valence region of the molecule. Table XI shows that calculations correlating 37 electrons reproduce the all-electron results.

## 2. Numerical stability of the finite field method

According to Eqs. (6) and (7), the  $W_d$  and  $W_s$  factors can be calculated as the first derivatives of the energy with respect to the corresponding perturbation. To calculate the derivative using numerical differentiation, it is necessary to determine the field strength at which the total energy depends linearly on the perturbation. Figure 5 shows the dependence of the total energy in  $\text{BaCH}_3$  on the  $\lambda_{d_c}$  perturbation. Linear behavior is found at smaller fields of the order of  $\lambda_{d_c} = 10^{-8}$  a.u. Similarly, for the  $W_s$  factor, the total energy is found to be linear at  $\lambda_{k_s} = 10^{-7}$  a.u. In  $\text{YbCH}_3$ ,  $\lambda_{d_c} = \lambda_{k_s} = 10^{-6}$  a.u. corresponds to the linear regime. To support these small fields, the convergence criterion of the coupled cluster energy as well as the Hartree-Fock energy was fixed at  $10^{-11}$  a.u.

- [1] G. Bertone, *Particle Dark Matter: Observations, Models and Searches* (Cambridge University Press, Cambridge, 2010).
- [2] J. Solà Peracaula, Cosmological constant and vacuum energy: Old and new ideas, *J. Phys. Conf. Ser.* **453**, 012015 (2013).
- [3] D. K. Barton, R. Falcone, D. Kleppner, F. K. Lamb, M. K. Lau, H. L. Lynch, D. Moncton, D. Montague, D. E. Mosher, W. Priedhorsky, M. Tigner, and D. R. Vaughan, Origin of the matter-antimatter asymmetry, *Rev. Mod. Phys.* **76**, S1 (2004).
- [4] J. Ginges and V. V. Flambaum, Violations of fundamental symmetries in atoms and tests of unification theories of elementary particles, *Phys. Rep.* **397**, 63 (2004).
- [5] Y. Yamaguchi and N. Yamanaka, Large Long-Distance Contributions to the Electric Dipole Moments of Charged Leptons in the Standard Model, *Phys. Rev. Lett.* **125**, 241802 (2020).
- [6] E. D. Commins, Electric dipole moments of leptons, in *Advances in Atomic, Molecular, and Optical Physics*, Vol. 40 (Elsevier, Amsterdam, 1999), pp. 1–55.
- [7] W. Bernreuther and M. Suzuki, The electric dipole moment of the electron, *Rev. Mod. Phys.* **63**, 313 (1991).
- [8] M. Pospelov and A. Ritz, CKM benchmarks for electron electric dipole moment experiments, *Phys. Rev. D* **89**, 056006 (2014).
- [9] M. Sachs and S. L. Schwebel, Implications of parity nonconservation and time reversal noninvariance in electromagnetic interactions: Part II. Atomic energy levels, *Ann. Phys.* **8**, 475 (1959).
- [10] E. Salpeter, Some atomic effects of an electronic electric dipole moment, *Phys. Rev.* **112**, 1642 (1958).
- [11] M. Bouchiat and C. Bouchiat, I. Parity violation induced by weak neutral currents in atomic physics, *J. Phys. France* **35**, 899 (1974).
- [12] P. Sandars, The electric dipole moment of an atom, *Phys. Lett.* **14**, 194 (1965).
- [13] P. Sandars, The electric-dipole moments of an atom II. the contribution from an electric-dipole moment on the electron with particular reference to the hydrogen atom, *J. Phys. B* **1**, 511 (1968).
- [14] P. Sandars, Measurability of the Proton Electric Dipole Moment, *Phys. Rev. Lett.* **19**, 1396 (1967).
- [15] D. DeMille, Diatomic molecules, a window onto fundamental physics, *Phys. Today* **68**, 34 (2015).
- [16] G. Harrison, P. Sandars, and S. Wright, Experimental Limit on the Proton Electric Dipole Moment, *Phys. Rev. Lett.* **22**, 1263 (1969).
- [17] E. Hinds, C. Loving, and P. Sandars, Limits on P and T violating neutral current weak interactions, *Phys. Lett. B* **62**, 97 (1976).
- [18] E. A. Hinds and P. G. H. Sandars, Experiment to search for P- and T-violating interactions in the hyperfine structure of thallium fluoride, *Phys. Rev. A* **21**, 480 (1980).
- [19] V. Andreev and N. Hutzler, (ACME Collaboration), Improved limit on the electric dipole moment of the electron, *Nature (London)* **562**, 355 (2018).
- [20] D. M. Kara, I. Smallman, J. J. Hudson, B. E. Sauer, M. R. Tarbutt, and E. A. Hinds, Measurement of the electron’s electric dipole moment using YbF molecules: Methods and data analysis, *New J. Phys.* **14**, 103051 (2012).
- [21] W. B. Cairncross, D. N. Gresh, M. Grau, K. C. Cossel, T. S. Roussy, Y. Ni, Y. Zhou, J. Ye, and E. A. Cornell, Precision Measurement of the Electron’s Electric Dipole Moment Using Trapped Molecular Ions, *Phys. Rev. Lett.* **119**, 153001 (2017).
- [22] R. F. Garcia Ruiz, R. Berger, J. Billowes, C. Binnersley, M. Bissell, A. Breier, A. Brinson, K. Chrysalidis, T. Coccolios, B. Cooper *et al.*, Spectroscopy of short-lived radioactive molecules, *Nature (London)* **581**, 396 (2020).
- [23] T. A. Isaev, S. Hoekstra, and R. Berger, Laser-cooled RaF as a promising candidate to measure molecular parity violation, *Phys. Rev. A* **82**, 052521 (2010).
- [24] P. Aggarwal, H. L. Bethlem, A. Borschevsky, M. Denis, K. Esajas, P. A. Haase, Y. Hao, S. Hoekstra, K. Jungmann, T. B.

- Meijknecht *et al.*, Measuring the electric dipole moment of the electron in BaF, *Eur. Phys. J. D* **72**, 197 (2018).
- [25] S. Bickman, P. Hamilton, Y. Jiang, and D. DeMille, Preparation and detection of states with simultaneous spin alignment and selectable molecular orientation in PbO, *Phys. Rev. A* **80**, 023418 (2009).
- [26] J. J. Hudson, D. M. Kara, I. Smallman, B. E. Sauer, M. R. Tarbutt, and E. A. Hinds, Improved measurement of the shape of the electron, *Nature (London)* **473**, 493 (2011).
- [27] I. Kozyryev and N. R. Hutzler, Precision Measurement of Time-Reversal Symmetry Violation with Laser-Cooled Polyatomic Molecules, *Phys. Rev. Lett.* **119**, 133002 (2017).
- [28] N. R. Hutzler, Polyatomic molecules as quantum sensors for fundamental physics, *Quantum Sci. Technol.* **5**, 044011 (2020).
- [29] A. M. Ellis, Main group metal-ligand interactions in small molecules: New insights from laser spectroscopy, *Intl. Rev. Phys. Chem.* **20**, 551 (2001).
- [30] T. Isaev, A. Zaitsevskii, and E. Eliav, Laser-coolable polyatomic molecules with heavy nuclei, *J. Phys. B: At., Mol. Opt. Phys.* **50**, 225101 (2017).
- [31] T. A. Isaev and R. Berger, Polyatomic Candidates for Cooling of Molecules with Lasers from Simple Theoretical Concepts, *Phys. Rev. Lett.* **116**, 063006 (2016).
- [32] I. Kozyryev, L. Baum, K. Matsuda, and J. M. Doyle, Proposal for laser cooling of complex polyatomic molecules, *Chem. Phys. Chem.* **17**, 3641 (2016).
- [33] D. Mitra, N. B. Vilas, C. Hallas, L. Anderegg, B. L. Augenbraun, L. Baum, C. Miller, S. Raval, and J. M. Doyle, Direct laser cooling of a symmetric top molecule, *Science* **369**, 1366 (2020).
- [34] B. L. Augenbraun, Z. D. Lasner, A. Frenett, H. Sawaoka, A. T. Le, J. M. Doyle, and T. C. Steimle, Observation and laser spectroscopy of ytterbium monomethoxide, YbOCH<sub>3</sub>, *Phys. Rev. A* **103**, 022814 (2021).
- [35] N. Shitara, N. Yamanaka, B. K. Sahoo, T. Watanabe, and B. P. Das, CP violating effects in 210fr and prospects for new physics beyond the standard model, *J. High Energy Phys.* **2** (2021) 124.
- [36] M. G. Kozlov and V. F. Ezhov, Enhancement of the electric dipole moment of the electron in the YbF molecule, *Phys. Rev. A* **49**, 4502 (1994).
- [37] P. A. B. Haase, D. J. Doeglas, A. Boeschoten, E. Eliav, M. Iliáš, P. Aggarwal, H. L. Bethlem, A. Borschevsky, K. Esajas, Y. Hao, S. Hoekstra, V. R. Marshall, T. B. Meijknecht, M. C. Mooij, K. Steinebach, R. G. E. Timmermans, A. P. Touwen, W. Ubachs, L. Willmann, and Y. Yin and (NL-eEDM Collaboration), Systematic study and uncertainty evaluation of P,T-odd molecular enhancement factors in BaF, *J. Chem. Phys.* **155**, 034309 (2021).
- [38] M. Denis, P. A. B. Haase, R. G. E. Timmermans, E. Eliav, N. R. Hutzler, and A. Borschevsky, Enhancement factor for the electric dipole moment of the electron in the BaOH and YbOH molecules, *Phys. Rev. A* **99**, 042512 (2019).
- [39] K. Gaul and R. Berger, *Ab initio* study of parity and time-reversal violation in laser-coolable triatomic molecules, *Phys. Rev. A* **101**, 012508 (2020).
- [40] A.-M. Mårtensson-Pendrill and P. Öster, Calculations of atomic electric dipole moments, *Phys. Scr.* **36**, 444 (1987).
- [41] H. D. Cohen and C. Roothaan, Electric dipole polarizability of atoms by the Hartree-Fock method. I. Theory for closed-shell systems, *J. Chem. Phys.* **43**, S34 (1965).
- [42] L. Visscher, T. Enevoldsen, T. Saue, and J. Oddershede, Molecular relativistic calculations of the electric field gradients at the nuclei in the hydrogen halides, *J. Chem. Phys.* **109**, 9677 (1998).
- [43] Y. Hao, M. Iliáš, E. Eliav, P. Schwerdtfeger, V. V. Flambaum, and A. Borschevsky, Nuclear anapole moment interaction in BaF from relativistic coupled-cluster theory, *Phys. Rev. A* **98**, 032510 (2018).
- [44] Y. Hao, P. Navrátil, E. B. Norrgard, M. Iliáš, E. Eliav, R. G. E. Timmermans, V. V. Flambaum, and A. Borschevsky, Nuclear spin-dependent parity-violating effects in light polyatomic molecules, *Phys. Rev. A* **102**, 052828 (2020).
- [45] P. A. B. Haase, E. Eliav, M. Iliáš, and A. Borschevsky, Hyperfine structure constants on the relativistic coupled cluster level with associated uncertainties, *J. Phys. Chem. A* **124**, 3157 (2020).
- [46] M. Denis, P. A. B. Haase, M. C. Mooij, Y. Chamorro, P. Aggarwal, H. L. Bethlem, A. Boeschoten, A. Borschevsky, K. Esajas, Y. Hao, S. Hoekstra, J. W. F. van Hofslot, V. R. Marshall, T. B. Meijknecht, R. G. E. Timmermans, A. Touwen, W. Ubachs, L. Willmann, and Y. Yin, Benchmarking of the Fock space coupled cluster method and uncertainty estimation: Magnetic hyperfine interaction in the excited state of BaF, *Phys. Rev. A* **105**, 052811 (2022).
- [47] M. G. Kozlov and L. N. Labzowsky, Parity violation effects in diatomics, *J. Phys. B: At., Mol. Opt. Phys.* **28**, 1933 (1995).
- [48] T. E. Chupp, P. Fierlinger, M. J. Ramsey-Musolf, and J. T. Singh, Electric dipole moments of atoms, molecules, nuclei, and particles, *Rev. Mod. Phys.* **91**, 015001 (2019).
- [49] A. S. P. Gomes, T. Saue, L. Visscher, H. J. Aa. Jensen, and R. Bast, with contributions from I. A. Aucar, V. Bakken, K. G. Dyall, S. Dubillard, U. Ekström, E. Eliav, T. Enevoldsen, E. Faßhauer, T. Fleig, O. Fossgaard, L. Halbert, E. D. Hedegård, B. Heimlich-Paris, T. Helgaker, J. Henriksson, M. Iliáš, Ch. R. Jacob, S. Knecht, S. Komorovský, O. Kullie, J. K. Lærdahl, C. V. Larsen, Y. S. Lee, H. S. Nataraj, M. K. Nayak, P. Norman, G. Olejniczak, J. Olsen, J. M. H. Olsen, Y. C. Park, J. K. Pedersen, M. Pernpointner, R. di Remigio, K. Ruud, P. Sałek, B. Schimmelpfennig, B. Senjean, A. Shee, J. Sikkema, A. J. Thorvaldsen, J. Thyssen, J. van Stralen, M. L. Vidal, S. Villaume, O. Visser, T. Winther, and S. Yamamoto, DIRAC, *A Relativistic Ab initio Electronic Structure Program*, Rel. DIRAC19 (2019), available at <https://doi.org/10.5281/zenodo.3572669>, see also <http://www.diracprogram.org>.
- [50] T. Saue, R. Bast, A. S. P. Gomes, H. J. A. Jensen, L. Visscher, I. A. Aucar, R. Di Remigio, K. G. Dyall, E. Eliav, E. Fasshauer *et al.*, The DIRAC code for relativistic molecular calculations, *J. Chem. Phys.* **152**, 204104 (2020).
- [51] J. F. Stanton, J. Gauss, L. Cheng, M. E. Harding, D. A. Matthews, P. G. Szalay, CFOUR, a quantum chemical program package, with contributions from A. Asthana, A. A. Auer, R. J. Bartlett, U. Benedikt, C. Berger, D. E. Bernholdt, S. Blaschke, Y. J. Bomble, S. Burger, O. Christiansen, D. Datta, F. Engel, R. Faber, J. Greiner, M. Heckert, O. Heun, M. Hilgenberg, C. Huber, T.-C. Jagau, D. Jonsson, J. Juslius, T. Kirsch, M.-P. Kitsaras, K. Klein, G. M. Kopper, W. J. Lauderdale, F. Lipparini, J. Liu, T. Metzroth, L. A. Mück, T. Nottoli, D. P. O'Neill, J. Oswald, D. R. Price, E. Prochnow, C. Puzzarini, K. Ruud, F. Schiffmann, W. Schwalbach, C. Simmons, S.

- Stopkowicz, A. Tajti, J. Vázquez, F. Wang, J. D. Watts, C. Zhang, X. Zheng and the integral packages MOLECULE (J. Almlöf and P. R. Taylor), PROPS (P. R. Taylor), ABACUS (T. Helgaker, H. J. Aa. Jensen, P. Jørgensen, and J. Olsen), and ECP routines by A. V. Mitin and C. van Wüllen. For the current version, see <http://www.cfour.de>.
- [52] D. A. Matthews, L. Cheng, M. E. Harding, F. Lipparini, S. Stopkowicz, T.-C. Jagau, P. G. Szalay, J. Gauss, and J. F. Stanton, Coupled-cluster techniques for computational chemistry: The program package, *J. Chem. Phys.* **152**, 214108 (2020).
- [53] L. Visscher, T. J. Lee, and K. G. Dyall, Formulation and implementation of a relativistic unrestricted coupled-cluster method including noniterative connected triples, *J. Chem. Phys.* **105**, 8769 (1996).
- [54] L. Visscher, E. Eliav, and U. Kaldor, Formulation and implementation of the relativistic Fock-space coupled cluster method for molecules, *J. Chem. Phys.* **115**, 9720 (2001).
- [55] K. G. Dyall, Relativistic double-zeta, triple-zeta, and quadruple-zeta basis sets for the 4s, 5s, 6s, and 7s elements, *J. Phys. Chem. A* **113**, 12638 (2009).
- [56] A. S. Gomes, K. G. Dyall, and L. Visscher, Relativistic double-zeta, triple-zeta, and quadruple-zeta basis sets for the lanthanides La–Lu, *Theor. Chem. Acc.* **127**, 369 (2010).
- [57] K. G. Dyall, Relativistic double-zeta, triple-zeta, and quadruple-zeta basis sets for the light elements H–Ar, *Theor. Chem. Acc.* **135**, 128 (2016).
- [58] B. O. Roos, V. Veryazov, and P.-O. Widmark, Relativistic atomic natural orbital type basis sets for the alkaline and alkaline-earth atoms applied to the ground-state potentials for the corresponding dimers, *Theor. Chem. Acc.* **111**, 345 (2004).
- [59] B. O. Roos, R. Lindh, P.-Å. Malmqvist, V. Veryazov, and P.-O. Widmark, Main group atoms and dimers studied with a new relativistic ANO basis set, *J. Phys. Chem. A* **108**, 2851 (2004).
- [60] B. O. Roos, R. Lindh, P.-Å. Malmqvist, V. Veryazov, P.-O. Widmark, and A. C. Borin, New relativistic atomic natural orbital basis sets for lanthanide atoms with applications to the ce diatom and LuF<sub>3</sub>, *J. Phys. Chem. A* **112**, 11431 (2008).
- [61] P.-O. Widmark, P.-Å. Malmqvist, and B. O. Roos, Density matrix averaged atomic natural orbital (ANO) basis sets for correlated molecular wave functions, *Theor. Chim. Acta* **77**, 291 (1990).
- [62] J. Xin, J. Robinson, A. Apponi, and L. M. Ziurys, High resolution spectroscopy of BaCH<sub>3</sub> ( $\tilde{X}^2A_1$ ): Fine and hyperfine structure analysis, *J. Chem. Phys.* **108**, 2703 (1998).
- [63] L. Schiff, Measurability of nuclear electric dipole moments, *Phys. Rev.* **132**, 2194 (1963).
- [64] L. Pašteka, R. Mawhorter, and P. Schwerdtfeger, Relativistic coupled-cluster calculations of the <sup>173</sup>Yb nuclear quadrupole coupling constant for the YbF molecule, *Mol. Phys.* **114**, 1110 (2016).
- [65] T. J. Lee and P. R. Taylor, A diagnostic for determining the quality of single-reference electron correlation methods, *Intl. J. Quantum Chem.* **36**, 199 (1989).
- [66] T. H. Dunning Jr., Gaussian basis sets for use in correlated molecular calculations. I. The atoms boron through neon and hydrogen, *J. Chem. Phys.* **90**, 1007 (1989).
- [67] D. Feller, Application of systematic sequences of wave functions to the water dimer, *J. Chem. Phys.* **96**, 6104 (1992).
- [68] T. Helgaker, W. Klopper, H. Koch, and J. Noga, Basis-set convergence of correlated calculations on water, *J. Chem. Phys.* **106**, 9639 (1997).
- [69] J. M. Martin, *Ab initio* total atomization energies of small molecules—Towards the basis set limit, *Chem. Phys. Lett.* **259**, 669 (1996).
- [70] M. Lesiuk and B. Jeziorski, Complete basis set extrapolation of electronic correlation energies using the Riemann zeta function, *J. Chem. Theory Comput.* **15**, 5398 (2019).
- [71] Y. Guo, L. F. Pašteka, E. Eliav, and A. Borschevsky, Ionization potentials and electron affinity of oganesson with relativistic coupled cluster method, in *Advances in Quantum Chemistry*, Vol. 83 (Elsevier, Amsterdam, 2021), pp. 107–123.
- [72] E. Lindroth, B. Lynn, and P. Sandars, Order  $\alpha^2$  theory of the atomic electric dipole moment due to an electric dipole moment on the electron, *J. Phys. B: At. Mol. Opt. Phys.* **22**, 559 (1989).
- [73] J. A. Gaunt, IV. The triplets of helium, *Philos. Trans. R. Soc. London A* **228**, 151 (1929).
- [74] C. Zhang, X. Zheng, and L. Cheng, Calculations of time-reversal-symmetry-violation sensitivity parameters based on analytic relativistic coupled-cluster gradient theory, *Phys. Rev. A* **104**, 012814 (2021).
- [75] V. S. Prasanna, N. Shitara, A. Sakurai, M. Abe, and B. P. Das, Enhanced sensitivity of the electron electric dipole moment from YbOH: The role of theory, *Phys. Rev. A* **99**, 062502 (2019).
- [76] R. F. Bader and T. Nguyen-Dang, Quantum theory of atoms in molecules—Dalton revisited, in *Advances in Quantum Chemistry*, Vol. 14 (Elsevier, Amsterdam, 1981), pp. 63–124.
- [77] E. D. Glendening, C. R. Landis, and F. Weinhold, NBO 6.0: Natural bond orbital analysis program, *J. Comput. Chem.* **34**, 1429 (2013).
- [78] J. P. Perdew, K. Burke, and M. Ernzerhof, Generalized Gradient Approximation Made Simple, *Phys. Rev. Lett.* **77**, 3865 (1996).
- [79] G. t. Te Velde, F. M. Bickelhaupt, E. J. Baerends, C. Fonseca Guerra, S. J. van Gisbergen, J. G. Snijders, and T. Ziegler, Chemistry with ADF, *J. Comput. Chem.* **22**, 931 (2001).
- [80] E. Espinosa, I. Alkorta, J. Elguero, and E. Molins, From weak to strong interactions: A comprehensive analysis of the topological and energetic properties of the electron density distribution involving X–H  $\cdots$  F–Y systems, *J. Chem. Phys.* **117**, 5529 (2002).
- [81] A. Sunaga, M. Abe, M. Hada, and B. P. Das, Analysis of large effective electric fields of weakly polar molecules for electron electric-dipole-moment searches, *Phys. Rev. A* **95**, 012502 (2017).
- [82] E. R. Meyer, J. L. Bohn, and M. P. Deskevich, Candidate molecular ions for an electron electric dipole moment experiment, *Phys. Rev. A* **73**, 062108 (2006).
- [83] N. R. Hutzler, H.-I. Lu, and J. M. Doyle, The buffer gas beam: An intense, cold, and slow source for atoms and molecules., *Chem. Rev.* **112**, 4803 (2012).
- [84] C. R. Brazier and P. F. Bernath, Observation of gas phase organometallic free radicals: Monomethyl derivatives of calcium and strontium, *J. Chem. Phys.* **86**, 5918 (1987).



- [85] A. Jadbabaie, N. H. Pilgram, J. Kłos, S. Kotochigova, and N. R. Hutzler, Enhanced molecular yield from a cryogenic buffer gas beam source via excited state chemistry, *New J. Phys.* **22**, 022002 (2020).
- [86] P. Yu and N. R. Hutzler, Probing Fundamental Symmetries of Deformed Nuclei in Symmetric Top Molecules, *Phys. Rev. Lett.* **126**, 023003 (2021).
- [87] Kei-ichi C. Namiki and T. C. Steimle, Pure rotational spectrum of  $\text{CaCH}_3(\tilde{X}^2A_1)$  using the pump/probe microwave-optical double resonance (PPMODR) technique, *J. Chem. Phys.* **110**, 11309 (1999).
- [88] P. M. Sheridan, M. J. Dick, J.-G. Wang, and P. F. Bernath, High-resolution spectroscopic investigation of the  $\tilde{B}^2A_1 - \tilde{X}^2A_1$  transitions of  $\text{CaCH}_3$  and  $\text{SrCH}_3$ , *J. Phys. Chem. A* **109**, 10547 (2005).
- [89] Kei-ichi C. Namiki, J. S. Robinson, and T. C. Steimle, A spectroscopic study of  $\text{caoch}_3$  using the pump/probe microwave and the molecular beam/optical stark techniques, *J. Chem. Phys.* **109**, 5283 (1998).
- [90] A. Petrov and A. Zakharova, Sensitivity of the yboh molecule to p t-odd effects in an external electric field, *Phys. Rev. A* **105**, L050801 (2022).
- [91] M. Iliaš and T. Saue, An infinite-order two-component relativistic hamiltonian by a simple one-step transformation, *J. Chem. Phys.* **126**, 064102 (2007).
- [92] T. Saue, Relativistic Hamiltonians for chemistry: A primer, *Chem. Phys. Chem.* **12**, 3077 (2011).
- [93] W. Zou, M. Filatov, and D. Cremer, Development and application of the analytical energy gradient for the normalized elimination of the small component method, *J. Chem. Phys.* **134**, 244117 (2011).